Research Article
Volume 10:3, 2021

Journal of
Applied & Computational Mathematics

ISSN: 2168-9679 Open Access

Heterogeneous-Homogeneous Reaction Mechanism on the Hydro Magneticnano Fluid Flow Over a Stretching Cylinder with Prescribed Heat Flux using Hermite Wavelet Method

Raghunatha KR[1]*, Kumbinarasaiah S[2]

[1]*Department of Mathematics, Davangere University, Davangere-577 007, India*
[2]*Department of Mathematics, Bangalore University, Bangalore-560 056, India*

Abstract

The current work provides the Hermite wavelet method (HWM) for an incompressible Nanofluid hydromagnetic flow through a stretching cylinder associated with heterogeneous-homogeneous chemical reactions. Single-walled carbon nanotubes (SWCNTs) with multi-walled carbon nanotubes (MWCNTs) as nanoparticles in the form of arranged heat flux are accounted for currently. Regulating equations, which are highly nonlinear coupled, are changed right into non-dimensional ordinary differential equations (ODEs) using appropriate similarity transformations. The desire for exceptional flow constraints on the flow feature is finalized truthfully through tables and graphs. Graphic summaries are offered for the rheological qualities of various parameters in size for velocity, temperature, concentrations, and nanoparticles. Comparison of the numerical outcomes is made with previously available consequences under particular cases, and the results are found to be in good agreement. The Hermite wavelet technique is hugely proficient and sensible for finding outcomes to this type of coupled nonlinear ODEs. The works are in outstanding accord for coupled nonlinear ordinary differential equations (ODEs) in engineering applications.

Keywords: Nonlinear differential equations • Operational matrix of integration • Collocation method • Hermite wavelets.

Introduction

The majority of the applied mathematics and engineering problems happen in highly nonlinear coupled differential equations. Several pertinent areas to wave phenomena enclose fluid mechanics, elastic media, plasma, optical fibres, etc. Also, obtaining accurate results for these problems is relatively unhurt. Nonetheless, in current years, numerical methods have drastically been urbanized to be used for a nonlinear coupled system of differential equations. A few of them were solved using different analytical and numerical methods.

The magnetic properties have significant uses in applied mathematics and engineering. For example, several manufacturing types of equipment, magnetohydrodynamic generators, bearings, pumps, and boundary layer manage are exaggerated by the contact involving the magnetic field and an electrically conducting fluid. The works of many researchers have been considered relative to these applications. One of the fundamental and significant issues around the hydromagnetic conduct of boundary layers is the length of fixed or moving surfaces within sight of a transverse magnetic field. The magnetic field and boundary layer problems are related in different industrial systems employing plasma flow transverse of magnetic fields and liquid metals [1]. Numerous scientists have contemplated the impacts of electrically conducting liquids, for example, fluid metals, water mixed with a little corrosive and different fixings within sight of an attractive field on the stream and warmth move of an incompressible gooey fluid disregarding a touching surface or an extending plate in an inactive liquid. Pavlov [2] was one of the principal pioneers in this field of study. Subsequently, a spearheading work by Pavlov [2], the flow past a moving level plate or an extending sheet within the transverse magnetic field has drawn thought, and a decent measure of writing has been produced on this problem ([3] and references therein).

From an energy-saving point of view, improvement of heat transfer execution in frameworks is an essential subject. The low thermal conductivity of regular heat transfer liquids, for example, water and oils, is a critical constraint for improving the exhibition and the compactness of frameworks. Solids usually have a higher warm conductivity than fluids. An imaginative and novel method to upgrade heat move is to utilize strong particles in the base liquid (for example, Nanofluids) in the scope of sizes 10–50 nm. However, in recent times Nanofluid [4], an innovative type of fluid categorize outstanding to fluid-solid understanding in non-metal or metal nanoparticle suspension; started by Choi [5], to heighten thermal conductivity of the fluid. Carbon nanotubes fundamentally are the cylinder of single or numerous sheets of grapheme. Fixated on grapheme sheets, carbon nanotubes are recognized into two kinds, viz. single and multiple-walled carbon nanotubes (SWCNTs and MWCNTs). For the most part, CNT is utilized in anodes, cathodes, impetus, and different clinical and natural applications because of its remarkable mechanical and electrical properties, just as flow conductivity. CNTs contain broad uses in aviation materials since they can likewise advance the reformist aviation materials' effects. A fluid system including CNT is exceptionally electrically conducting, suggesting that they may safeguard airplane from the lightning strike. Ample literature can be found on CNTs flow problems ([6-8] and and references therein). Sheikholeslami [9] studied the support of fixed suction occurrence on Nano fluid flow during cylinder and calculated efficient thermal conductivity in adding viscosity by KKL system. Kardri et al. [10] considered heat transfer and flow features during cylinder and recognize that the dual result exists for stretching cylinder. Nadeem et al. [11] investigated the individuality of 3D stagnation-point hybrid-Nano fluid flow during cylinder and established that heat transfer rate is advanced in hybrid Nano fluid than Nano fluid.

Heat flux is characterized as the pace transfer of heat energy during a predefined surface. Numerous scientists [12-14] exhibit flow and heat broadcast overextending cylinder utilizing recommended heat transition. Alavi et al. [15] studied endorsed heat motion to catch the quality of MHD flow over a dramatically extending sheet. Heat transfer examination utilizing recommended heat motion through stretching sheet was reviewed by Majeed et al. [15].

***Address for Correspondence:** Raghunatha KR, Department of Mathematics, Davangere University, Davangere-577 007, India, Tel: 8095810145; E-mail: raghunatha13@davangereuniversity.ac.in; raghunatha13@gmail.com*

Received 17 February 2021; **Accepted** 19 March 2021; **Published** 26 March 2021

In various manufacturing developed, burning, paint fabricating, biomedical creation, food handling, and metal deliberation from commonly discovered mineral, homogeneous, heterogeneous synthetic responses happen. Bachok et al. [17] examined stagnation flow in the form of heterogeneous-homogeneous compound response over a growing surface by allowing for indistinguishable dispersion pace of reactant and auto catalyst. Muhammad et al. [18] investigated boundary layer Ferro-hydrodynamic flow within sight of heterogeneous-homogeneous responses. Newly, Nano fluid flow with heterogeneous-homogeneous reactions was concentrated by Kumar et al. [19].

Practically all arithmetical modelling involves linear or nonlinear differential equations. To determine those equations impeccably, approximately, or mathematically a few specialists employ various excellent scientific, semi-analytic plans alongside lasting label of convergence. There are different mathematical techniques to solve such nonlinear differential equations; however, a few significant information counting circular occurrence determination be misplaced throughout the process of finding the solution. Hence, analytical techniques contain emerged to solve highly nonlinear differential equations such as the

Homotopy Analysis Method (HAM) [20,21], Homotopy Analysis Sumudu Transform Method (HASTM) [22], Homotopy Perturbation Method [23,24], Variational Iteration Method[25-27], q- Homotopy Analysis Transform Method (q-HAM) [28], Energy Balance Method [29,30], new extended direct algebraic method [31,32], Homotopy Analysis Transform Method (HATM) [33], Differential Transformation Method (DTM) [34,35], Exp-function Method [36-38] and Akbari-Ganji's Method [39].

To the very best of our understanding, no study was performed in an incompressible Nano fluidhydro magnetic flow during stretching cylinders associated with heterogeneous- homogeneous chemical reactions by using the wavelet technique. Wavelet theory is one of the recent emerging approaches in applied mathematics. It has a wide range of applications in the following fields as Signal analyses, computer science, mathematical modeling, image processing, and applied sciences. Many mathematicians' contributions towards wavelets based numerical methods are as follows: Laguerre wavelets method [40], Hermite wavelets method [41], B-spline approach [42], Wavelet collocation method [43], Generalized Hermite wavelets method [44], etc. SWCNTs and MWCNTs as nanoparticles in the look of set heat transfer motion are considered here. It has significant uses in anodes, cathodes, semiconductors, microelectronics, paper creation, glass blowing, plastic sheets, polymer preparation, food handling, ignition, aviation materials, paint industry, and mechanical different clinical and biomedical innovation, and ecological investigations. The numerical simulations have been employed using a numerical method recognized as HWM (see, for details, [41]. The Velocity and temperature distribution are advanced in MWCNT than SWCNT, and the opposite trend could be seen for concentration circulations presented in tables and graphs. The results gotten are compared to the earlier findings, which are in excellent agreement with the current work. It is expected that modern literary works will undoubtedly offer better details for the science and industrial sectors.

The organization of this paper is as follows; section 2 is devoted to the problem formulation. The progress of the Hermite matrix of integration is available in section 3. Section 4 reveals the method of solution, and the results are discussed in section 5. Finally, the conclusion is drawn in section 6.

Problem formulation

The basic highly nonlinear coupled ordinary differential equations (ODEs), which described in an incompressible nanofluid hydro magnetic flow through stretching cylinder associated with heterogeneous- homogeneous chemical reaction, can be summarized as introduced by ShankarGeri et al. [45]:

$$(1+2\gamma t)f'''+2\gamma f''+(1-\phi)^{2.5}\left\{\left[(1-\phi)+\phi\left(\frac{\rho_{CNT}}{\rho_f}\right)\right]\left[f f''-(f')^2\right]-\mathrm{M}\, f'\right\}=0 \quad (2.1)$$

$$\frac{\kappa_{nf}/\kappa_f}{\left[(1-\phi)+\phi\dfrac{(\rho C_p)_{CNT}}{(\rho C_p)_f}\right]}\left\{(1+2\gamma t)\theta''+2\gamma\theta'\right\}+Pr\left(f\theta'-f'\theta\right)=0 \quad (2.2)$$

$$\frac{1}{Sc}\left\{(1+2\gamma t)g''+2\gamma g'\right\}+f g'-\lambda g G^2=0 \quad (2.3)$$

$$\frac{\delta}{Sc}\left\{(1+2\gamma t)G''+2\gamma G'\right\}+f G'+\lambda g G^2=0 \quad (2.4)$$

$$\left.\begin{array}{l} f(0)=0, f'(0)=1, \theta'(0)=-1, g'(0)=K_s g(0), \delta G'(0)=-K_s g(0) \\ f'(t)\to 0,\ \theta(t)\to 0,\ g(t)\to 1,\ G(t)\to 0 \quad \text{as} \quad t\to\infty \end{array}\right\}. \quad (2.5)$$

Where the prime (') represents differentiation with respect to *t*.

Without loss of generality, we suppose that the molecular diffusion rates of chemical species *A* and *B* are of a similar size. Besides, we think that $D_A = D_B$, i.e. $\delta = 1$; so we believe from the hypothesis that $g(t) + G(t) = 1$. Thus, (2.3) and (2.4) gather together to

$$(1+2\gamma t)g''+2\gamma g'+Sc\, f g'-\lambda\, Sc\, g(1-g)^2=0 \quad (2.6)$$

With the rehabilitated boundary conditions

$$\left.\begin{array}{l} f(0)=0, f'(0)=1, \theta'(0)=-1, g'(0)=K_s g(0) \\ f'(t)\to 0,\ \theta(t)\to 0,\ g(t)\to 1,\ \text{as} \quad t\to\infty \end{array}\right\} \quad (2.7)$$

Hermite wavelet operation matrix of integration

Hermite wavelet

Hermite wavelets are defined in detail (Shiralashetti and Kumbinarasaiah [42]).

Approximation of function

We would approximate $y(x)$ under Hermite space by elements of Hermite wavelet basis as follows:

$$y(x)=\sum_{n=1}^{\infty}\sum_{m=0}^{\infty}C_{m,n}\phi_{m,n}(x), \quad (3.1)$$

Where $\phi_{m,n}(x)$ is given in (3.1).

We approximate $y(x)$ by truncating the series as follows

$$y(x)\approx\sum_{m=1}^{2^{k-1}}\sum_{n=0}^{N-1}C_{m,n}\,\phi_{m,n}(x)=A^T\phi(x), \quad (3.2)$$

Where*A* and $\phi(x)$ are $2^{k-1}N\times 1$ matrix,

$$A^T=[C_{1,0},\dots C_{1,N-1},C_{2,0}\dots C_{2,N-1},\dots C_{2^{k-1},0},\dots C_{2^{k-1},N-1}],$$

$$\phi(x)=[\phi_{1,0},\dots\phi_{1,N-1},\phi_{2,0},\dots\phi_{2,N-1},\dots\phi_{2^{k-1},0},\dots\phi_{2^{k-1},N-1}]^T.$$

Operational matrix

Operational matrix of integration

Here, we extracted some Hermite wavelet basis at *k* = 1 as follows:

$$\phi_{1,0}(x)=\frac{2}{\sqrt{\pi}}$$

$$\phi_{1,1}(x)=\frac{1}{\sqrt{\pi}}(8x-4)$$

$$\phi_{1,2}(x)=\frac{1}{\sqrt{\pi}}(32x^2-32x+4)$$

$$\phi_{1,3}(x)=\frac{1}{\sqrt{\pi}}(128x^3-192x^2+48x+8)$$

$$\phi_{1,4}(x)=\frac{1}{\sqrt{\pi}}(512x^4-1024x^3+384x^2+128x-40)$$

$$\phi_{1,5}(x)=\frac{1}{\sqrt{\pi}}(2048x^5-5120x^4+2560x^3+1280x^2-800x+16)$$

$$\phi_{1,6}(x)=\frac{1}{\sqrt{\pi}}(8192x^6-24576x^5+15360x^4+10240x^3-9600x^2+384x+368)$$

$$\phi_{1,7}(x)=\frac{1}{\sqrt{\pi}}(32768x^7-114688x^6+86016x^5+71680x^4-89600x^3+5376x^2+10304x-928)$$

$$\phi_{1,8}(x)=\frac{1}{\sqrt{\pi}}(131072x^8-524288x^7+458752x^6+458752x^5-716800x^4+ 57344x^3+164864x^2-29696x-3296)$$

$$\phi_{1,9}(x)=\frac{1}{\sqrt{\pi}}(524288x^9-2359296x^8+2359296x^7+2752512x^6-5160960x^5+516096x^4+ 1978368x^3-534528x^2-118656x+21440)$$

$$\phi_{1,10}(x)=\frac{1}{\sqrt{\pi}}(2097152x^{10}-10485760x^9+11796480x^8+15728640x^7-34406400x^6+ 4128768x^5+19783680x^4-7127040x^3-2373120x^2+857600x+16448)$$

$$\phi_{1,11}(x)=\frac{1}{\sqrt{\pi}}(8388608x^{11}-46137344x^{10}+57671680x^9+86507520x^8-216268800x^7+ 30277632x^6+174096384x^5-78397440x^4-34805760x^3+18867200x^2+723712x-461696)$$

$$\phi_{1,12}(x)=\frac{1}{\sqrt{\pi}}(33554432x^{12}-201326592x^{11}+276824064x^{10}+461373440x^9-1297612800x^8+207618048x^7+ 1392771072x^6-752615424x^5-417669120x^4+301875200x^3+17369088x^2-22161408x+561536)$$

Where,

$$\phi_9(x)=[\phi_{1,0}(x),\phi_{1,1}(x),\phi_{1,2}(x),\phi_{1,3}(x),\phi_{1,4}(x),\phi_{1,5}(x),\phi_{1,6}(x),\phi_{1,7}(x),\phi_{1,8}(x)]^T$$

Now integrate above first nine basis concerning *x* limit from 0 to *x*, then express as a linear combination of Hermite wavelet basis as,

$$\int_0^x \phi_{1,0}(x)=\begin{bmatrix}\frac{1}{2} & \frac{1}{4} & 0 & 0 & 0 & 0 & 0 & 0 & 0\end{bmatrix}\phi_9(x)$$

$$\int_0^x \phi_{1,1}(x)=\begin{bmatrix}\frac{-1}{4} & 0 & \frac{1}{8} & 0 & 0 & 0 & 0 & 0 & 0\end{bmatrix}\phi_9(x)$$

$$\int_0^x \phi_{1,2}(x)=\begin{bmatrix}\frac{-1}{3} & 0 & 0 & \frac{1}{12} & 0 & 0 & 0 & 0 & 0\end{bmatrix}\phi_9(x)$$

$$\int_0^x \phi_{1,3}(x)=\begin{bmatrix}\frac{5}{4} & 0 & 0 & 0 & \frac{1}{16} & 0 & 0 & 0 & 0\end{bmatrix}\phi_9(x)$$

$$\int_0^x \phi_{1,4}(x)=\begin{bmatrix}\frac{-2}{5} & 0 & 0 & 0 & 0 & \frac{1}{20} & 0 & 0 & 0\end{bmatrix}\phi_9(x)$$

$$\int_0^x \phi_{1,5}(x)=\begin{bmatrix}\frac{-23}{3} & 0 & 0 & 0 & 0 & 0 & \frac{1}{24} & 0 & 0\end{bmatrix}\phi_9(x)$$

$$\int_0^x \phi_{1,6}(x)=\begin{bmatrix}\frac{116}{7} & 0 & 0 & 0 & 0 & 0 & 0 & \frac{1}{28} & 0\end{bmatrix}\phi_9(x)$$

$$\int_0^x \phi_{1,7}(x)=\begin{bmatrix}\frac{103}{2} & 0 & 0 & 0 & 0 & 0 & 0 & 0 & \frac{1}{32}\end{bmatrix}\phi_9(x)$$

$$\int_0^x \phi_{1,8}(x)=\begin{bmatrix}\frac{-2680}{9} & 0 & 0 & 0 & 0 & 0 & 0 & 0 & 0\end{bmatrix}\phi_9(x)+\frac{1}{36}\phi_{1,9}(x)$$

Hence,

$$\int_0^x \phi(x)\,dx=H_{9\times 9}\;\phi_9(x)+\overline{\phi_9}(x)$$

Where,

$$H_{9\times 9}=\begin{bmatrix}\frac{1}{2} & \frac{1}{4} & 0 & 0 & 0 & 0 & 0 & 0 & 0\\ \frac{-1}{4} & 0 & \frac{1}{8} & 0 & 0 & 0 & 0 & 0 & 0\\ \frac{-1}{3} & 0 & 0 & \frac{1}{12} & 0 & 0 & 0 & 0 & 0\\ \frac{5}{4} & 0 & 0 & 0 & \frac{1}{16} & 0 & 0 & 0 & 0\\ \frac{-2}{5} & 0 & 0 & 0 & 0 & \frac{1}{20} & 0 & 0 & 0\\ \frac{-23}{3} & 0 & 0 & 0 & 0 & 0 & \frac{1}{24} & 0 & 0\\ \frac{116}{7} & 0 & 0 & 0 & 0 & 0 & 0 & \frac{1}{28} & 0\\ \frac{103}{2} & 0 & 0 & 0 & 0 & 0 & 0 & 0 & \frac{1}{32}\\ \frac{-2680}{9} & 0 & 0 & 0 & 0 & 0 & 0 & 0 & 0\end{bmatrix},\ \overline{\phi_9}(x)=\begin{bmatrix}0\\0\\0\\0\\0\\0\\0\\0\\ \frac{1}{36}\phi_{1,9}(x)\end{bmatrix}.$$

Next, twice integration of above nine basis is given below

$$\int_0^x\int_0^x \phi_{1,0}(x)\,dxdx=\begin{bmatrix}\frac{3}{16} & \frac{1}{8} & \frac{1}{32} & 0 & 0 & 0 & 0 & 0 & 0\end{bmatrix}\phi_9(x)$$

$$\int_0^x\int_0^x \phi_{1,1}(x)\,dxdx=\begin{bmatrix}\frac{-1}{6} & \frac{-1}{16} & 0 & \frac{1}{96} & 0 & 0 & 0 & 0 & 0\end{bmatrix}\phi_9(x)$$

$$\int_0^x\int_0^x \phi_{1,2}(x)\,dxdx=\begin{bmatrix}\frac{-1}{16} & \frac{-1}{12} & 0 & 0 & \frac{1}{192} & 0 & 0 & 0 & 0\end{bmatrix}\phi_9(x)$$

$$\int_0^x\int_0^x \phi_{1,3}(x)\,dxdx=\begin{bmatrix}\frac{3}{5} & \frac{5}{16} & 0 & 0 & 0 & \frac{1}{320} & 0 & 0 & 0\end{bmatrix}\phi_9(x)$$

$$\int_0^x\int_0^x \phi_{1,4}(x)\,dxdx=\begin{bmatrix}\frac{-7}{12} & \frac{-1}{10} & 0 & 0 & 0 & 0 & \frac{1}{480} & 0 & 0\end{bmatrix}\phi_9(x)$$

$$\int_0^x\int_0^x \phi_{1,5}(x)\,dxdx=\begin{bmatrix}\frac{-22}{7} & \frac{-23}{12} & 0 & 0 & 0 & 0 & 0 & \frac{1}{672} & 0\end{bmatrix}\phi_9(x)$$

$$\int_0^x\int_0^x \phi_{1,6}(x)\,dxdx=\begin{bmatrix}\frac{81}{8} & \frac{29}{7} & 0 & 0 & 0 & 0 & 0 & 0 & \frac{1}{896}\end{bmatrix}\phi_9(x)$$

$$\int_0^x\int_0^x \phi_{1,7}(x)\,dxdx=\begin{bmatrix}\frac{148}{9} & \frac{103}{8} & 0 & 0 & 0 & 0 & 0 & 0 & 0\end{bmatrix}\phi_9(x)+\frac{1}{1152}\phi_{1,9}(x)$$

$$\int_0^x\int_0^x \phi_{1,8}(x)\,dxdx=\begin{bmatrix}\frac{-773}{5} & \frac{-670}{9} & 0 & 0 & 0 & 0 & 0 & 0 & 0\end{bmatrix}\phi_9(x)+\frac{1}{1440}\phi_{1,10}(x)$$

Hence,

$$\int_0^x\int_0^x \phi(x)\,dxdx=H'_{9\times 9}\;\phi_9(x)+\overline{\phi'_9}(x)$$

Where,

$$H'_{9\times 9}=\begin{bmatrix}\frac{3}{16} & \frac{1}{8} & \frac{1}{32} & 0 & 0 & 0 & 0 & 0 & 0\\ \frac{-1}{6} & \frac{-1}{16} & 0 & \frac{1}{96} & 0 & 0 & 0 & 0 & 0\\ \frac{-1}{16} & \frac{-1}{12} & 0 & 0 & \frac{1}{192} & 0 & 0 & 0 & 0\\ \frac{3}{5} & \frac{5}{16} & 0 & 0 & 0 & \frac{1}{320} & 0 & 0 & 0\\ \frac{-7}{12} & \frac{-1}{10} & 0 & 0 & 0 & 0 & \frac{1}{480} & 0 & 0\\ \frac{-22}{7} & \frac{-23}{12} & 0 & 0 & 0 & 0 & 0 & \frac{1}{672} & 0\\ \frac{81}{8} & \frac{29}{7} & 0 & 0 & 0 & 0 & 0 & 0 & \frac{1}{896}\\ \frac{148}{9} & \frac{103}{8} & 0 & 0 & 0 & 0 & 0 & 0 & 0\\ \frac{-773}{5} & \frac{-670}{9} & 0 & 0 & 0 & 0 & 0 & 0 & 0\end{bmatrix},\ \overline{\phi'_9}(x)=\begin{bmatrix}0\\0\\0\\0\\0\\0\\0\\ \frac{1}{1152}\phi_{1,9}(x)\\ \frac{1}{1440}\phi_{1,10}(x)\end{bmatrix}$$

Again triple integration of above nine basis is given by,

$$\int_0^x\int_0^x\int_0^x \phi_{1,0}(x)\,dxdxdx=\begin{bmatrix}\frac{5}{96} & \frac{3}{64} & \frac{1}{64} & \frac{1}{384} & 0 & 0 & 0 & 0 & 0\end{bmatrix}\phi_9(x)$$

$$\int_0^x\int_0^x\int_0^x \phi_{1,1}(x)\,dxdxdx=\begin{bmatrix}\frac{-7}{128} & \frac{-1}{24} & \frac{-1}{128} & 0 & \frac{1}{1536} & 0 & 0 & 0 & 0\end{bmatrix}\phi_9(x)$$

$$\int_0^x\int_0^x\int_0^x \phi_{1,2}(x)\,dxdxdx=\begin{bmatrix}\frac{-1}{80} & \frac{-1}{64} & \frac{-1}{96} & 0 & 0 & \frac{1}{3840} & 0 & 0 & 0\end{bmatrix}\phi_9(x)$$

$$\int_0^x\int_0^x\int_0^x \phi_{1,3}(x)\,dxdxdx=\begin{bmatrix}\frac{19}{96} & \frac{3}{20} & \frac{5}{128} & 0 & 0 & 0 & \frac{1}{7680} & 0 & 0\end{bmatrix}\phi_9(x)$$

$$\int_0^x\int_0^x\int_0^x \phi_{1,4}(x)\,dxdxdx=\begin{bmatrix}\frac{-13}{56} & \frac{-7}{48} & \frac{-1}{80} & 0 & 0 & 0 & 0 & \frac{1}{13440} & 0\end{bmatrix}\phi_9(x)$$

$$\int_0^x\int_0^x\int_0^x \phi_{1,6}(x)\,dxdxdx=\begin{bmatrix}\frac{133}{36} & \frac{81}{32} & \frac{29}{56} & 0 & 0 & 0 & 0 & 0 & 0\end{bmatrix}\phi_9(x)+\frac{1}{32256}\phi_{1,9}(x)$$

$$\int_0^x\int_0^x\int_0^x \phi_{1,6}(x)\,dxdxdx=\begin{bmatrix}\frac{133}{36} & \frac{81}{32} & \frac{29}{56} & 0 & 0 & 0 & 0 & 0 & 0\end{bmatrix}\phi_9(x)+\frac{1}{32256}\phi_{1,9}(x)$$

$$\int_0^x\int_0^x\int_0^x \phi_{1,7}(x)\,dxdxdx=\begin{bmatrix}\frac{193}{40} & \frac{37}{9} & \frac{103}{64} & 0 & 0 & 0 & 0 & 0 & 0\end{bmatrix}\phi_9(x)+\frac{1}{46080}\phi_{1,10}(x)$$

$$\int_0^x\int_0^x\int_0^x \phi_{1,8}(x)\,dxdxdx=\begin{bmatrix}\frac{-1211}{22} & \frac{-773}{20} & \frac{-335}{36} & 0 & 0 & 0 & 0 & 0 & 0\end{bmatrix}\phi_9(x)+\frac{1}{46080}\phi_{1,11}(x)$$

Hence,

$$\int_0^x\int_0^x\int_0^x \phi(x)\,dxdxdx = H''_{9\times 9}\ \phi_9(x) + \overline{\phi}''_9(x)$$

where,

$$H''_{9\times9} = \begin{bmatrix} \frac{5}{96} & \frac{3}{64} & \frac{1}{64} & \frac{1}{384} & 0 & 0 & 0 & 0 & 0 \\ \frac{-7}{128} & \frac{-1}{24} & \frac{-1}{128} & 0 & \frac{1}{1536} & 0 & 0 & 0 & 0 \\ \frac{-1}{80} & \frac{-1}{64} & \frac{-1}{96} & 0 & 0 & \frac{1}{3840} & 0 & 0 & 0 \\ \frac{19}{96} & \frac{3}{20} & \frac{5}{128} & 0 & 0 & 0 & \frac{1}{7680} & 0 & 0 \\ \frac{-13}{56} & \frac{-7}{48} & \frac{-1}{80} & 0 & 0 & 0 & 0 & \frac{1}{13440} & 0 \\ \frac{-65}{64} & \frac{-11}{14} & \frac{-23}{96} & 0 & 0 & 0 & 0 & 0 & \frac{1}{21504} \\ \frac{133}{36} & \frac{81}{32} & \frac{29}{56} & 0 & 0 & 0 & 0 & 0 & 0 \\ \frac{193}{40} & \frac{37}{9} & \frac{103}{64} & 0 & 0 & 0 & 0 & 0 & 0 \\ \frac{-1211}{22} & \frac{-773}{20} & \frac{-335}{36} & 0 & 0 & 0 & 0 & 0 & 0 \end{bmatrix}, \overline{\phi}''_9(x) = \begin{bmatrix} 0 \\ 0 \\ 0 \\ 0 \\ 0 \\ 0 \\ \frac{1}{32256}\phi_{1,9}(x) \\ \frac{1}{46080}\phi_{1,10}(x) \\ \frac{1}{63360}\phi_{1,11}(x) \end{bmatrix}$$

In the same way, we can create matrices for our convenience. In the result section, the third-order highly nonlinear coupled ordinary differential equations are solved using N=6 and 9. So, we generated matrices of order 9*9 up to a triple operational matrix of integration.

Method of solution

Now, assume that

$$f'''(x) = A^T\psi(x) \tag{4.1}$$

Integrate Eq. (4.1) with respect to *x* form 0 to *x*,we get,

$$f''(x) = f''(0) + A^T\left[P\psi(x) + \overline{\psi}(x)\right] \tag{4.2}$$

Integrate (4.2) with respect to *x* form 0 to *x*

$$f'(x) = f'(0) + x\,f''(0) + A^T\left[P'\psi(x) + \overline{\psi}'(x)\right] \tag{4.3}$$

Integrate (4.3) concerning *x* form 0 to *x*

$$f(x) = f(0) + x\,f'(0) + \frac{x^2}{2}f''(0) + A^T\left[P''\psi(x) + \overline{\psi}''(x)\right] \tag{4.4}$$

$$f(x) = x + \frac{x^2}{2}f''(0) + A^T\left[P''\psi(x) + \overline{\psi}''(x)\right] \tag{4.5}$$

Put $x=\eta$ in (4.3) we get

$$f'(\eta) = 1 + \eta\,f''(0) + A^T\left[P'\psi(x) + \overline{\psi}'(x)\right]\Big|_{x=\eta} \tag{4.6}$$

$$f''(0) = \frac{1}{\eta}\left\{-1 - A^T\left[P'\psi(x) + \overline{\psi}'(x)\right]\right\}\Big|_{x=\eta} \tag{4.7}$$

Fit (4.7) in (4.2, 4.3, 4.5) we get

$$f''(x) = \frac{1}{\eta}\left\{-1 - A^T\left[P'\psi(x) + \overline{\psi}'(x)\right]\right\}\Big|_{x=\eta} + A^T\left[P\psi(x) + \overline{\psi}(x)\right] \tag{4.8}$$

$$f'(x) = 1 + \frac{x}{\eta}\left\{-1 - A^T\left[P'\psi(x) + \overline{\psi}'(x)\right]\right\}\Big|_{x=\eta} + A^T\left[P'\psi(x) + \overline{\psi}'(x)\right] \tag{4.9}$$

$$f(x) = x + \frac{x^2}{2}\frac{1}{\eta}\left\{-1 - A^T\left[P'\psi(x) + \overline{\psi}'(x)\right]\right\}\Big|_{x=\eta} + A^T\left[P''\psi(x) + \overline{\psi}''(x)\right] \tag{4.10}$$

Again put

$$\theta''(x) = B^T\psi(x) \tag{4.11}$$

Integrate (4.11) with respect to *x* form 0 to *x*

$$\theta'(x) = -1 + B^T\left[P\psi(x) + \overline{\psi}(x)\right] \tag{4.12}$$

Integrate (4.12) concerning *x* form 0 to *x*

$$\theta(x) = \theta(0) - x + B^T\left[P'\psi(x) + \overline{\psi}'(x)\right] \tag{4.13}$$

Put $x=\eta$ in the above equation, we get

$$\theta(\eta) = \theta(0) - \eta + B^T\left[P'\psi(x) + \overline{\psi}'(x)\right]\Big|_{x=\eta} \tag{4.14}$$

$$\theta(0) = \eta - B^T\left[P'\psi(x) + \overline{\psi}'(x)\right]\Big|_{x=\eta} \tag{4.15}$$

Form (4.15) and (4.13), we get

$$\theta(x) = \eta - B^T\left[P'\psi(x) + \overline{\psi}'(x)\right]\Big|_{x=\eta} - x + B^T\left[P'\psi(x) + \overline{\psi}'(x)\right] \tag{4.16}$$

Again put

$$g''(x) = C^T\psi(x) \tag{4.17}$$

Integrate (4.17) concerning *x* form 0 to *x*

$$g'(x) = g'(0) + C^T\left[P\psi(x) + \overline{\psi}(x)\right] = K_s g(0) + C^T\left[P\psi(x) + \overline{\psi}(x)\right] \tag{4.18}$$

Integrate (4.18) concerning *x* form 0 to *x*

$$g(x) = g(0) + K_s g(0)x + C^T\left[P'\psi(x) + \overline{\psi}'(x)\right] \tag{4.19}$$

Put $x=\eta$ in the above equation, we get

$$g(\eta) = g(0)[1 + K_s\,\eta] + C^T\left[P'\psi(x) + \overline{\psi}'(x)\right]\Big|_{x=\eta} \tag{4.20}$$

$$g(0) = \frac{1}{[1 + K_s\,\eta]}\left(1 - C^T\left[P'\psi(x) + \overline{\psi}'(x)\right]\Big|_{x=\eta}\right) \tag{4.21}$$

form (4.21) and (4.18), (4.19) we get

$$g'(x) = K_s\frac{1}{[1 + K_s\,\eta]}\left(1 - C^T\left[P'\psi(x) + \overline{\psi}'(x)\right]\Big|_{x=\eta}\right) + C^T\left[P\psi(x) + \overline{\psi}(x)\right] \tag{4.22}$$

$$g(x) = \frac{[1 + K_s\,x]}{[1 + K_s\,\eta]}\left(1 - C^T\left[P'\psi(x) + \overline{\psi}'(x)\right]\Big|_{x=\eta}\right) + C^T\left[P'\psi(x) + \overline{\psi}'(x)\right] \tag{4.23}$$

Again put

$$G''(x) = D^T\psi(x) \tag{4.24}$$

Integrate (4.24) concerning *x* form 0 to *x*

$$G'(x) = G'(0) + D^T\left[P\psi(x) + \overline{\psi}(x)\right] = -\frac{K_s}{\delta}g(0) + D^T\left[P\psi(x) + \overline{\psi}(x)\right] \tag{4.25}$$

$$G'(x) = -\frac{K_s}{\delta}\frac{1}{[1 + K_s\,\eta]}\left(1 - C^T\left[P'\psi(x) + \overline{\psi}'(x)\right]\Big|_{x=\eta}\right) + D^T\left[P\psi(x) + \overline{\psi}(x)\right] \tag{4.26}$$

Integrate (4.26) concerning *x* form 0 to *x*

$$G(x) = G(0) - \frac{K_s}{\delta}\frac{x}{[1 + K_s\,\eta]}\left(1 - C^T\left[P'\psi(x) + \overline{\psi}'(x)\right]\Big|_{x=\eta}\right) + D^T\left[P'\psi(x) + \overline{\psi}'(x)\right] \tag{4.27}$$

Put $x=\eta$ in the above equation, we get

$$G(\eta) = G(0) - \frac{K_s}{\delta}\frac{\eta}{[1 + K_s\,\eta]}\left(1 - C^T\left[P'\psi(x) + \overline{\psi}'(x)\right]\Big|_{x=\eta}\right) + D^T\left[P'\psi(x) + \overline{\psi}'(x)\right]\Big|_{x=\eta} \tag{4.28}$$

$$G(0) = \frac{K_s}{\delta}\frac{\eta}{[1 + K_s\,\eta]}\left(1 - C^T\left[P'\psi(x) + \overline{\psi}'(x)\right]\Big|_{x=\eta}\right) - D^T\left[P'\psi(x) + \overline{\psi}'(x)\right]\Big|_{x=\eta} \tag{4.29}$$

form (4.29) and (4.27), we get

$$G(x) = \frac{K_s}{\delta}\frac{\eta}{[1 + K_s\,\eta]}\left(1 - C^T\left[P'\psi(x) + \overline{\psi}'(x)\right]\Big|_{x=\eta}\right) - D^T\left[P'\psi(x) + \overline{\psi}'(x)\right]\Big|_{x=\eta} - \frac{K_s}{\delta}\frac{x}{[1 + K_s\,\eta]}\left(1 - C^T\left[P'\psi(x) + \overline{\psi}'(x)\right]\Big|_{x=\eta}\right) + D^T\left[P'\psi(x) + \overline{\psi}'(x)\right] \tag{4.30}$$

Substitute $f''', f'', f', f, g'', g', g, \theta'', \theta', \theta, G'', G', G$ in a given system of highly nonlinear coupled ODEs. Then collate each ODE by the following collocation points $x_i = \frac{2i-1}{2N}$. Where $i = 1, 2, 3, \cdots, N$ and

Nrepresents the size of the operational matrix. Then we get a nonlinear algebraic equations system and solve this system by Newton's method that yields the Hermite wavelet's unknown coefficients. Substitute these unknown coefficients to f, θ, g and G will reflect the Laguerre wavelet-based numerical solutions for a given system of nonlinear coupled ODEs.

Results and Discussions

To find the Hermite wavelet functional matrix method's efficiency, we solved highly nonlinear coupled ordinary differential equations and compared the calculated outcomes with other methods available in the literature. From Table 2, we compare the Runge-Kutta method, Finite difference method, DTM, and HWM methods when $M=\gamma=\phi=0$ and in the nonexistence of a chemical reaction. Hence we can be fulfilled that HWM is a more suitable method for solving highly nonlinear coupled ODEs (2.1–2.5). The physical behaviour of different known physical parameters in the confirmed flow problem on the velocity, temperature, and concentration fields is presented in Figures 1-10.

The velocity curves for different values of curvature parameter γ are presented in Figure 1. We noticeable the increase in fluid velocity during growth. Temperature dispersionbecause of curvature parameter γhave been depicted in Figure 2. Temperature dispersionenhances like velocity profiles for increasing γ. Velocity and temperature curves are superior in MWCNT than SWCNT. The concentration curves (Figure 3) support an undefined way like temperature curves when γheightens and afterward concentration boundary layers obtain thicker. The velocity curves for different values of nanoparticle concentration ϕ are presented in Figure 4. We evident the improvement in liquid velocity for increasing ϕ and henceforth impetus boundary layer gets thicker. Figure 5 shows that the temperature curves for various nanoparticle concentration values ϕ, and it uncovered that temperature curves increase with the increase in ϕ. This choice with an actual component that ϕ increases shows thermal conductivity quickens and in like manner thermal boundary layer width gets increased. Velocity

Table 1. The dimensionless parameters are introduced in equations (2.1-2.5).

Definition	Notation	Parameter
$\left(\frac{\nu_f L}{U_0}\right)^{0.5}$	γ	curvature parameter
$\frac{D_B}{D_A}$	δ	the ratio of the mass diffusion coefficient
$\frac{\mu_f (C_p)_f}{\kappa_f}$	*Pr*	Prandtl number
$\frac{\nu_f}{D_A}$	*Sc*	Schmidt number
$\frac{k_1 a_0^2 L}{U_0}$	λ	Homogeneous chemical reaction factor
$\frac{k_s}{D_A}\sqrt{\frac{\nu_f L}{U_0}}$	K_s	Heterogeneous chemical reaction factor
$\frac{\sigma_{nf} B_0^2 L}{\rho_f U_0}$	M	Revised magnetic parameter

Table 2. Variation of $\theta(0)$ for different values of *Pr*.

Pr	Bachok and Ishak [14]	Elbashbeshy [13]	SankarGiri et al. [45]	Present Method	
				HWM (N=6)	HWM(N=12)
0.72	1.2367	1.2253	1.236582	1.20374	1.23667
1.00	1.0000	1.0000	0.999999	0.98872	1.00000
6.70	0.3333	-	0.333303	0.30131	0.33331
10.0	0.2688	0.2688	0.268768	0.27621	0.26887

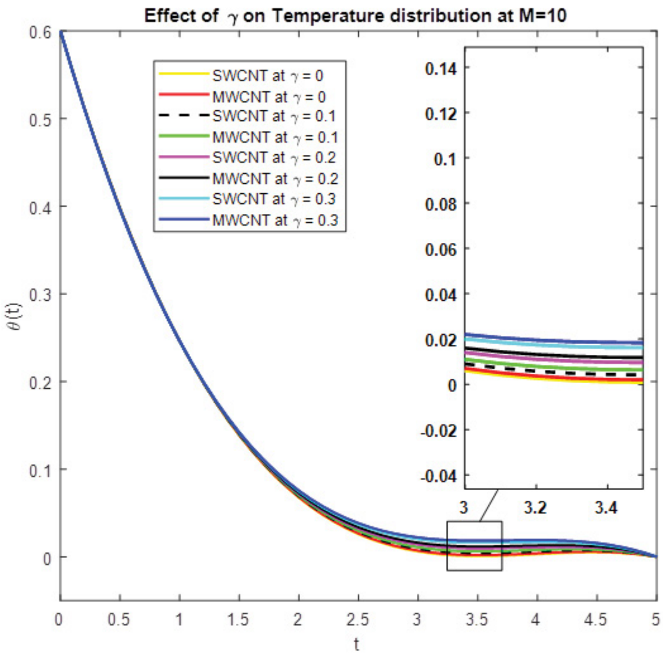

Figure 1. Velocity curves for different values of curvature parameter.

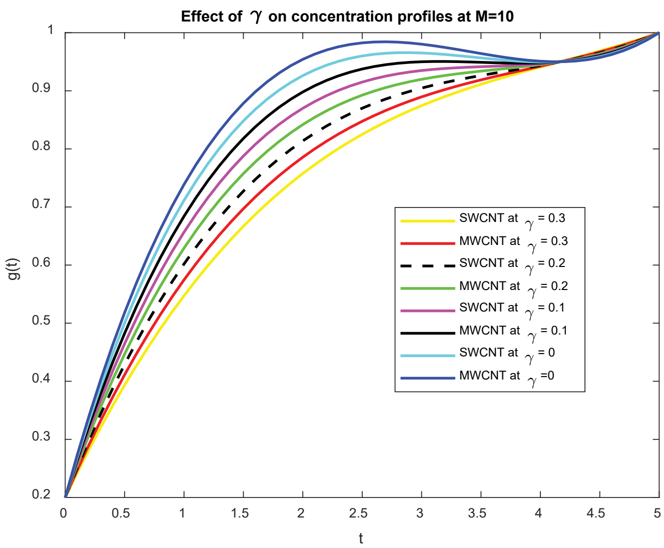

Figure 2. Temperature curves for different values of curvature parameter.

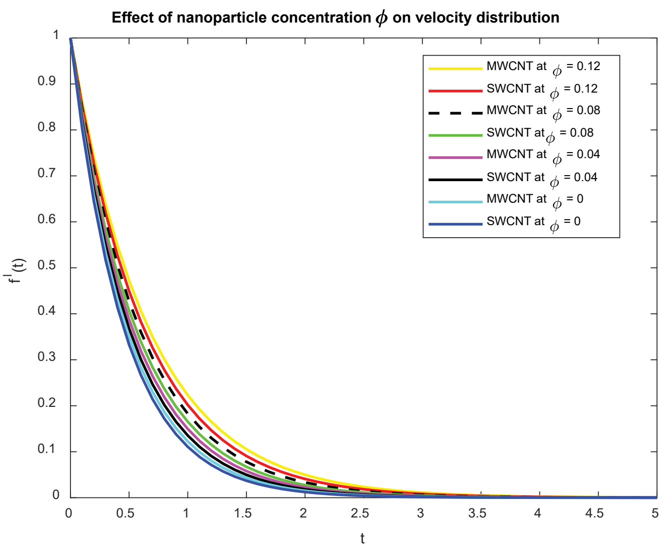

Figure 3. Concentration curves for different values of curvature parameter.

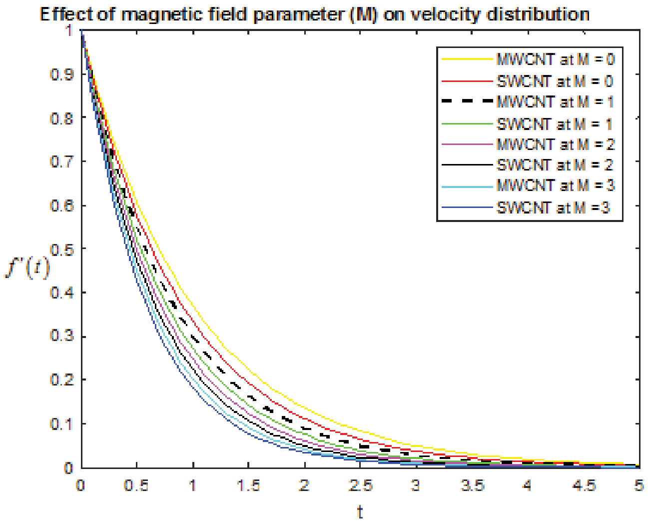

Figure 4. Velocity curves for different values of nanoparticle concentration.

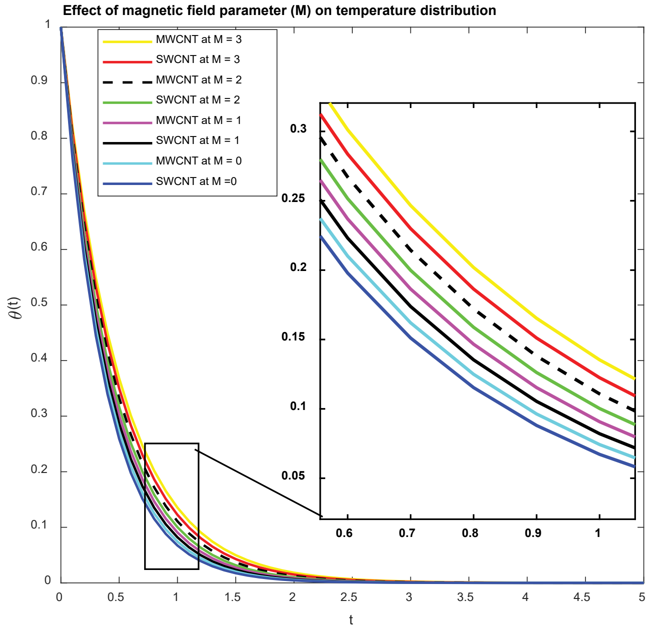

Figure 7. Temperature curves for different values of the magneticfield parameter.

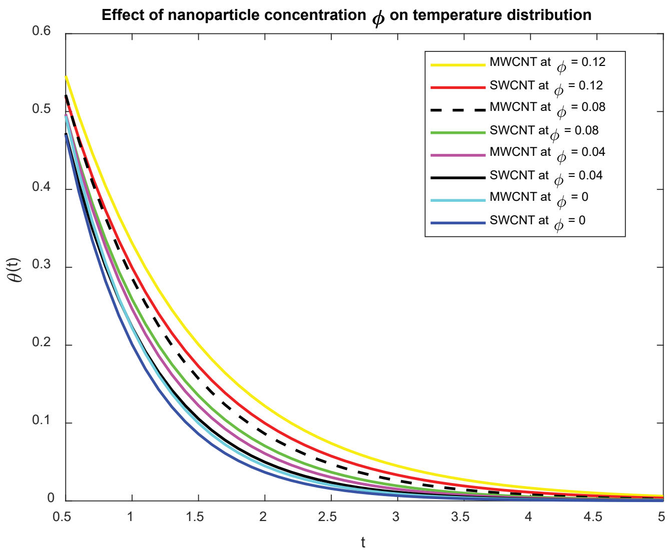

Figure 5. Temperature curves for different values of nanoparticle concentration.

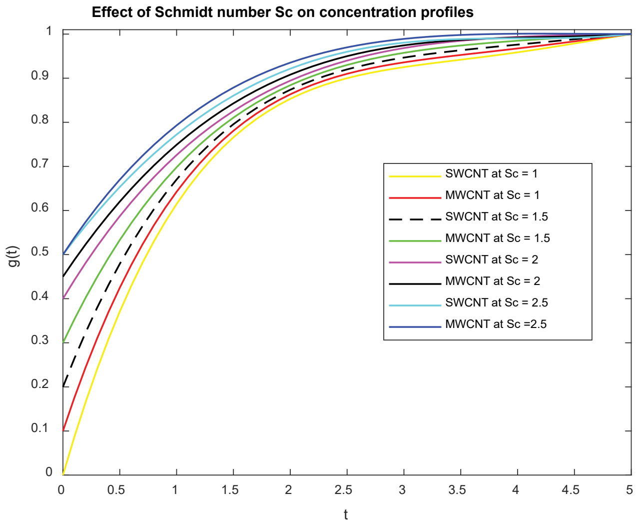

Figure 8. Concentration curves for different values of Schmidt number.

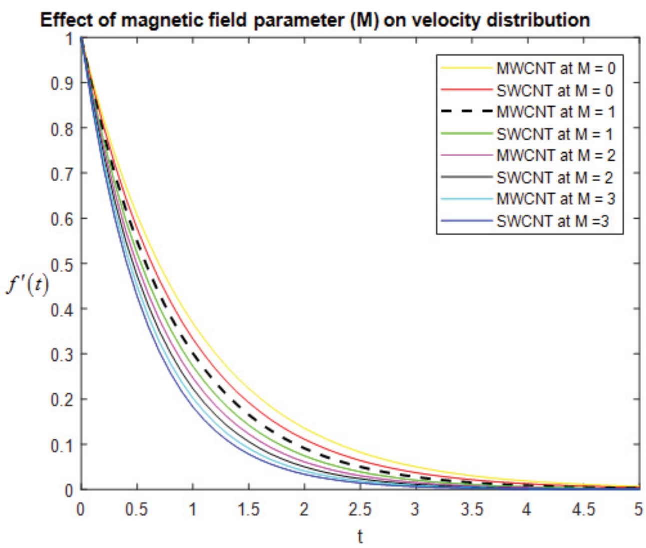

Figure 6. Velocity curves for different values of the magneticfield parameter.

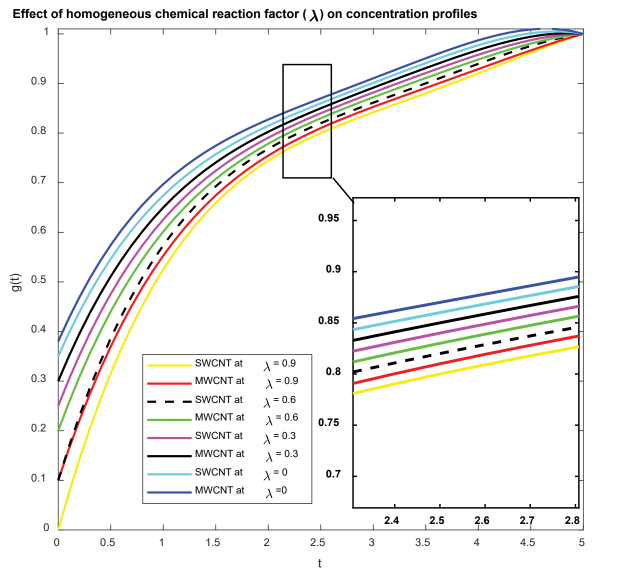

Figure 9. Concentration curves for different values of homogeneous chemical reaction factor.

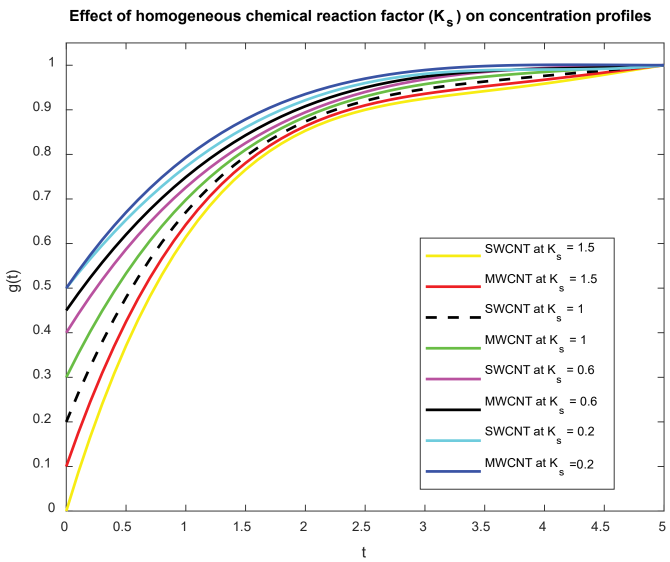

Figure 10. Concentration curves for different values of heterogeneous chemical reaction factor.

and temperature curves are advanced in MWCNT than SWCNT. The velocity curves for different values of the magnetic-field parameter M are presented in Figure 6. The graphical agreement embraces the rejection of liquid speed while the potency of the magnetic field gets engorged. Figure 7 revealed how magnetic-field parameter M follows up on temperature field. We comprehend that temperature dispersion is supported with M. While extra work total needed to loosen up nanofluid contrary to the magnetic field's purpose, heats transport nanofluid and improve temperature curves. Velocity and temperature curves are advanced in MWCNT than SWCNT. Schmidt number is perceived as a proportion of the rate of momentum diffusivity to the rate of mass diffusivity; thus, higher estimations of *Sc* suggest little mass distribution and as an aftereffect concentration curves refute, which are depicted in Figure 8. Concentration curves are superior in SWCNT than MWCNT. Uniform chemical reaction factor λ intensifies the spices *B*, which balanced nanoparticles in it. Like this nanoparticles' creation upgrades. This legitimizes that g is increased in the scheme as explained in Figure 9. In Figure 10, we reveal the thump of heterogeneous chemical reaction factor (K_s) on the flow. The first-order heterogeneous response happens in the endurance of solid engrossing warmed heated surface, which absorbs *A* and *B* and afterward a reply happens and following flavours *B* emerged from the divider thermally energizing nanoparticle in it. Consequently g upturns. Concentration curves are greater in SWCNT than MWCNT.

Conclusion

This manuscript enlarges heterogeneous-homogeneous chemical reaction in an incompressible nanofluid hydromagnetic flow through a stretching cylinder. SWCNTs, as well as MWCNTs nanoparticles, are considered at this point. We reformed coupled PDEs to couple highly nonlinear ODEs using the similarity technique and then resolved by HWM. The outcome process of HWM shows the competence of HWM for solving highly nonlinear differential equations, which is shown in the tables and figures. The computed solution via this technique is close to a numerical solution. Moreover, the HWM is more capable than any numerical method to solve this type of equations. The critical outcomes of the foregoing study may be summarized as follows:

The velocity curves are the same for different values γ and ϕ.

Temperature curves are improved with γ, M, and ϕ.

Velocity and temperature curves are advanced in MWCNT than SWCNT, and opposite results are seen in the case of concentration curves.

Concentration curves increase for chemical reaction factor.

References

1. Liron N, Wilhelm HE. "Integration of the magneto-hydrodynamic boundary layer equations by Meksyn's method." *J Appl Math Mech* 54 (1974):27-37.
2. Pavlov KB. "Magneto hydrodynamic flow of an incompressible viscous fluid caused by deformation of a plane surface." *Magnitnaya Gidrodinamika* 4 (1974): 146-147.
3. Ishak Anuar, Nazar Roslinda and Pop Ioan. "Magneto hydrodynamic (MHD) flow and heat transfer due to a stretching cylinder." *Energy Conversion and Management* 49(2008):3265-3269.
4. Mondal Hiranmoy, Almakki Mohammed and Sibanda Precious. "Dual solutions for three-dimensional magneto hydrodynamic nanofluid flow with entropy generation." *J Comput Des Eng* 6(2019): 657–665.
5. Choi S. "U. S. Developments and application of non-Newtonian flows, New York." USA: *ASME Press* (1995).
6. Ahmed Z and Nadeem S. "Flow of a micro polar CNT-based nanofluid across a squeezing channel." *Physica Scripta* 94(2019):10.
7. ST Hussain, Haq Rizwan-ul, ZH Khan and S Nadeem. "Water-driven flow of carbon nanotubes in a rotating channel." *J Mol Liq* 214 (2016): 136–144.
8. ShahzadiIqra, S Nadeem, Rabiei Faranak. "Simultaneous effects of single wall carbon nanotube and effective variable viscosity for peristaltic flow through annulus having permeable walls." *Results in Physics* 7 (2017): 667-676.
9. M Sheikholeslami. "Effect of uniform suction on nanofluid flow and heat transfer over a cylinder." The Brazilian Society of Mechanical Sciences and Engineering 37 (2015):1623-1633.
10. Kardri Mahani Ahmad, Bachok Norfifah, Arifin Norihan Md and AliFadzilah Md. "Boundary layer flow and heat transfer over a stretching cylinder in a copper water nanofluid." *American Institute of Physics* 1795 (2017): 020012.
11. S Nadeem, Nadeem Abbas. "AU Characteristics of three-dimensional stagnation point flow of a hybrid nanofluid past a circular cylinder." Results in Physics 8(2018): 829-835
12. Munawar Sufian, Mehmood Ahmer and Ali Asif. "Time-dependent flow and heat transfer over stretching cylinder." *Chin J Phys* 50(2012): 828-848.
13. Elbashbeshy Elsayed MAE. "Heat transfer over a stretching surface with variable surface heat flux." *J Phys D J Phys D Appl Phys* 31(1998): 1951-1954.
14. Bachok Norfifah, Ishak Anuar. "Flow and heat transfer over a stretching cylinder with prescribed surface heat flux." *Malaysian J Math Sci* 4(2010):159-169.
15. Alavi Sayed Qasim, Hussanan Abid, Kasim Abdul Rahman Mohd and Rosli Norhayati, et al. "MHD stagnation point flow towards an exponentially stretching sheet with prescribed wall temperature and heat flux." *Int J Appl Math Comput Sci* 3(2017): 3511-3523.
16. Majeed A, Zeeshan A and Ellahi R. "Unsteady ferromagnetic liquid flow and heat transfer analysis over a stretching sheet with the effect of dipole and prescribed heat flux." *J Mol Liq 22* (2016): 528-533.
17. Bachok Norfifah, Ishak Anuar. "PopIoan, On the stagnation-point flow towards a stretching sheet with homogeneous–heterogeneous reactions effects." Communication in Nonlinear Science and Numerical Simulation 16 (2011): 4296-4302.
18. Muhammad Noor, Nadeem S, Mustafa MT. "Hybrid isothermal model for the ferrohydrodynamic chemically reactive species." Communication in Theoretical Physics 71 (2019): 384-392.

19. Kumar Rakesh, Sood Shilpa, Sheikholeslami Mohsen and Shehzad Sabir Ali. "Nonlinear thermal radiation and cubic autocatalysis chemical reaction effects on the flow of stretched nanofluid under rotational oscillations." *J Colloid Interface Sci* 505 (2017)253265.

20. Fakhari A, Domairry Ganji and Ebrahimpour. "Approximate explicit solutions of nonlinear BBMB equations by homotopy analysis method and comparison with the exact solution." *Physics Letters A* 368(2007): 64-68.

21. Ganji DD and Fazeli M. "Homotopy analysis method to determine the fin effciency of convective straight fins with temperature dependent thermal conductivity." *Communications in Nonlinear Science and Numerical Simulation* 14 (2009): 489-499.

22. Devendra Kumar, Singh Jagdev and Baleanu Dumitru. "Numerical computation of a fractional model of differential-difference equation." *J Comput Nonlinear Dyn 11*(2016): 061004.

23. Hei-Huan. "Homotopy perturbation technique." *Comp Meth App Mech Eng* 178 (1999): 257-262.

24. Sheikholeslami M, Ashorynejad HR, Ganji DD and Yıldırım A. "Homotopy perturbation method for three-dimensional problem of condensation film on inclinedrotating disk." *Scientia Iranica* 19 (2012): 437-442.

25. Samaee SS, Yazdanpanah O and Ganji DD. "New approaches to identification of the Lagrange multiplier in the Variational Iteraton Method." *J Braz Soc Mech Sci Engin* 37(2015): 937-944.

26. Mohyud-Din, Syed Tauseef, Aslam Noor Muhammad and Noor KI. "Variational Iteration Method for Re-formulated Partial Differential Equations." *Int J Nonlinear Sci Numer Simul* 11(2011): 87-92.

27. Mohyud-Din Syed Tauseef, Aslam Noor Muhammad, Noor KI. "Some Relatively New Techniques for Nonlinear Problems." *Mathematical Problems in Engineering* 25 (2009).

28. Jagdev Singh, Kumar Devendra and Swroop Ram. "Numerical solution of timeand space-fractional coupled Burgers' equations via homotopy algorithm." Alexandria Engineering J 55(2016):1753-1763.

29. Momeni M, Jamshidi N, Barari A and Ganji DD. "Application of He's energy balance method to Duffing-harmonic oscillators." *Int J Comput Math* 88(2011): 135-144.

30. Mehdipour I, Ganji DD and Mozaffari M. "Application of the energy balance method to nonlinear vibrating equations." *Current Applied Physics* 10(2010): 104-112.

31. Rezazadeh Hadi, Osman MS, Eslami Mustafa and Mirzazadeh Mohammad. "Hyperbolic rational solutions to a variety of conformable fractional Boussinesq-Like equations." Nonlinear *Engineering* 8(2019): 224-230.

32. Rezazadeh Hadi, Mirhosseini-Alizamini, Seyed Mehdi and Eslami Mostafa. "New optical solitons of nonlinear conformable fractional Schrödinger-Hirota equation." *Optik* 172(2018):545-553.

33. Kumar Devendra,Singh Jagdev,Kumar Sunil and Sing P. "Numerical computation of nonlinear shockwave equation of fractional order." *Ain Shams Eng J* 6 (2015): 605-611.

34. Sheikholeslami Mohsen and Ganji Davood Domiri. "Nanofluid flow and heat transfer between parallel plates considering Brownian motion using DTM." Computer Methods in Applied Mechanics and Engineering 283 (2015): 651-663.

35. Zhou LK. "Differential Transformation and Its Applications for Electrical Circuits, Huazhong University Press, Wuhan, (1986).

36. Noor Muhammad Aslam, Mohyud-DinSyed Tauseef and Waheed Asif, Al-Said. "Exp-function method for traveling wave solutions of nonlinear evolution equations." Applied Mathematics and Computation 216 (2015): 477-483.

37. Noor Muhammad Aslam, Mohyud-Din Syed Tauseef and Waheed Asif. "Exp-function method for generalized traveling solutions of master partial differential equations." Acta Applicandae Mathematicae, Springer 104(2008): 131-137.

38. Mohyud-Din Syed Tauseef, Noor Muhammad Aslam and Waheed Asif. "Exp-function method for generalized traveling solutions of Calogero-Degasperis-Fokas equation, Zeitschrift für Naturforschung" A- *J Phys Sci* 65a (2010):78-84.

39. Talarposhti RA , Asadi Z, Rezazadeh H Ganji and Bekir A. "Analytical solution for differential nonlinear and coupled equations in micropolar nanofluid flow between rotating parallel plates." *Eur Phys J Spec* 228(12) (2019): 2601-2617.

40. Shiralashetti SC and Kumbinarasaiah S. Theoretical study on continuous polynomial wavelet bases through wavelet series collocation method for nonlinear Lane–Emden type equations." *Appl Math Comput* 315(2017):591-602.

41. Shiralashetti SC and Kumbinarasaiah S. "Hermite wavelets operational matrix of integrationfor the numerical solution of nonlinear singularinitial value problems." *Alex Eng J* 57(2018): 2591-2600.

42. Shiralashetti SC and Kumbinarasaiah S. "Cardinal B-Spline Wavelet-Based Numerical Method for the Solution of Generalized Burgers–Huxley Equation." *Int J Appl Comput Math* 4 (2018): 73.

43. Shiralashetti SC and Kumbinarasaiah S. "Laguerre wavelets collocation method for the numerical solution of the Benjamina–Bona–Mohany equations." *J Taibah Uni Sci* 13 (2019): 9-15.

44. Shiralashetti SC and Kumbinarasaiah S. "New generalized operational matrix of integrationfor solves nonlinear singular boundary value problems using Hermite wavelets." *Arab J Basic Appl Sci* 26(2019): 385-396.

45. Sankar Giri Shib, Das Kalidas and Kundu Prabir Kumar. "Homogeneous–heterogeneous reaction mechanism on MHD carbon nanotube flow over a stretching cylinder with prescribed heat flux using differential transform method." *J Comput Des Eng* 7(3) (2020): 337-351.

How to cite this article: Raghunatha KR, Kumbinarasaiah S. Heterogeneous-Homogeneous Reaction Mechanism on the Hydro Magneticnano Fluid Flow Over a Stretching Cylinder with Prescribed Heat Flux using Hermite Wavelet Method. *J Appl Computat Math* 10 (2021): 466.